Use of Multidimensional Fiber Grating Strain Sensors for Damage Detection in Composite Pressure Vessels

Marley Kunzler[a], Eric Udd
Blue Road Research, 376 NE 219th Avenue, Gresham, OR 97030

Mont Johnson and Kurt Mildenhall
ATK Thiokol, PO Box 707, M/S 252, Brigham City, Utah 84302

ABSTRACT

Arrays of multi-axis fiber grating strain sensors have been integrated into a composite pressure vessel test article, and are used to monitor changes in the transverse and axial strain fields during curing and pressure cycling near cut tow and Teflon tape defects. These changes in the multi-axis strain due to four pressure cycles and repeated impacts are measured and compared to ultrasonic and eddy current scans. Examples of the remote detection of damage using transverse strain and transverse strain gradients is given as well as data showing the ability of the system to distinguish broken tow and delamination defects.

INTRODUCTION

Multi-axis fiber grating strain sensors[1-3] have been used to measure transverse strain, shear strain, pressure, and other key parameters. In composite materials, they may also be used to measure transverse strain gradients and enable a new approach to determining both the character of damage and its location. This paper overviews the usage of arrays of multi-axis fiber grating strain sensors in a subscale demonstration article. The signatures obtained from cut tow and manufactured delaminations simulated by disks of Teflon tape appear distinctly different. Strain-induced damage can be detected through composite layers, behind optical fiber and at distances of several centimeters. By implementing a read-out system with arrays containing large numbers of fiber grating strain sensors, it is possible to develop a “strain imaging” system to be used to identify the location and extent of damage in a composite.

MULTI-AXIS FIBER GRATING STRAIN SENSORS

An axial-strain measuring fiber grating strain sensor can be expanded into a multi-axis strain sensor by using polarization maintaining (PM), or birefringent optical fiber. The residual stress created in the birefringent fiber during manufacturing results in a slight change in the index of refraction along two mutually orthogonal polarization axes. This creates two spectral peaks for each

Report Documentation Page

Form Approved
OMB No. 0704-0188

1. REPORT DATE	2. REPORT TYPE	3. DATES COVERED
MAR 2004		**-**

4. TITLE AND SUBTITLE	5a. CONTRACT NUMBER
Use of Multidimensional Fiber Grating Strain Sensors for Damage Detection in Composite Pressure Vessels	**F04611-02-C-0007**
	5b. GRANT NUMBER
	5c. PROGRAM ELEMENT NUMBER

6. AUTHOR(S)	5d. PROJECT NUMBER
Marley Kunzler; Eric Udd; Mont Johnson; Kurt Mildenhall	**3005**
	5e. TASK NUMBER **02AG**
	5f. WORK UNIT NUMBER

7. PERFORMING ORGANIZATION NAME(S) AND ADDRESS(ES)	8. PERFORMING ORGANIZATION REPORT NUMBER
Blue Road Research,Clear Creek Business Park,376 NE 219th Avenue,Gresham,OR,97030	

9. SPONSORING/MONITORING AGENCY NAME(S) AND ADDRESS(ES)	10. SPONSOR/MONITOR'S ACRONYM(S)
	11. SPONSOR/MONITOR'S REPORT NUMBER(S)

12. DISTRIBUTION/AVAILABILITY STATEMENT

Approved for public release; distribution unlimited

13. SUPPLEMENTARY NOTES

14. ABSTRACT

Arrays of multi-axis fiber grating strain sensors have been integrated into a composite pressure vessel test article, and are used to monitor changes in the transverse and axial strain fields during curing and pressure cycling near cut tow and Teflon tape defects. These changes in the multi-axis strain due to four pressure cycles and repeated impacts are measured and compared to ultrasonic and eddy current scans. Examples of the remote detection of damage using transverse strain and transverse strain gradients is given as well as data showing the ability of the system to distinguish broken tow and delamination defects.

15. SUBJECT TERMS

16. SECURITY CLASSIFICATION OF:			17. LIMITATION OF ABSTRACT	18. NUMBER OF PAGES	19a. NAME OF RESPONSIBLE PERSON
a. REPORT	b. ABSTRACT	c. THIS PAGE			
unclassified	**unclassified**	**unclassified**		**12**	

optical grating written into the optical fiber, one associated with each polarization axis, for each single fiber grating.

As the fiber is transversely loaded, the relative index of refraction of the polarization axes of the fiber change and the net result is a difference in wavelength between the spectral peaks. When the fiber is strained axially--depending on the situation, the fiber either elongates or compresses, changing the fiber grating spectral period and the output spectrum to longer or shorter wavelengths, respectively.

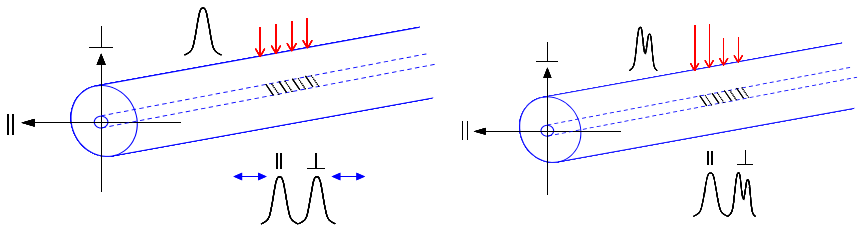

Figure 1. Uneven strain loading on a multi-axis fiber grating causes peak-splitting

Figure 1a illustrates a multi-axis grating written onto polarization preserving fiber, which is subject to a uniform transverse load. In this case, the two spectral reflection peaks, corresponding to the effective fiber gratings along each birefringent (polarization) axis, move apart or together uniformly providing a means to measure transverse strain. In the case where load along the transverse axis is not uniform, as shown in Figure 1b, the peak associated with the non-uniform transverse load splits. The transverse strain gradient is measured quantitatively by the spectral separation between the peaks. The portion of the grating under a fixed transverse load is reflected in the amplitude of the peak. For example, in Figure 1a the transverse load along the vertical axis is uniform. There are only two spectral peaks as a result, and their spectral separation defines the transverse load. In the case of Figure 1b, the transverse load has two values along the vertical axis, each along approximately one half of the fiber grating length. In this case, the spectral peak corresponding to the vertical axis splits. The spectral shift between these sub-peaks determines the transverse load gradient. As an example, in this case a shift of 0.1 nm corresponds to approximately 300 με (microstrain). The amplitudes of the two split peaks are approximately equal, which indicates that each of the two distinct transverse load regions are approximately equal. (The amplitude of the fiber grating spectral peak indicates the fraction of the fiber grating under that load.) The wavelength peak response of the fiber to transverse strain correlates to approximately 1/3 of response to axial strain along the length of the fiber.

The axes of these fiber sensors may be aligned optically to within a few degrees of rotational angle and tabbed for insertion into composite parts including the cylindrical pressure bottle described in this paper.

PLACEMENT OF SENSORS IN DEMONSTRATION ARTICLE

The demonstration article was divided into four quadrants shown in Figure 2. Quadrant 1 contained twenty 1300 nm (center wavelength) dual-axis fiber Bragg grating strain sensors, as well as four dual-axis 1550 nm senors. The sensors were positioned around either a band of cut-filament composite fibers (cut bands or cut tow), or Teflon tape disks embedded into the part to cause delamination defects. Both cut band defects were manufactured into the cylindrical sections of the bottle while one of the Teflon tape defects was placed in the cylinder with a second defect placed in one of the domes. Quadrants 2 and 4 were designed as buffer zones between damage areas and did not contain known defects or embedded sensors. Quadrant 3 contained two simulated arrays; one array positioned in the dome section and one in the cylinder section of the bottle. These arrays mirrored the arrays of Quadrant 1.

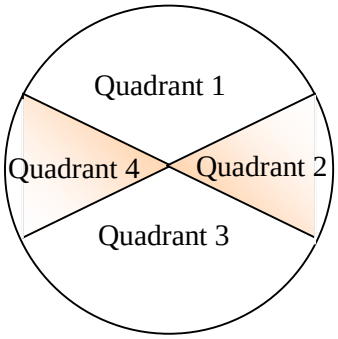

Figure 2. The cylindrical bottle was divided into test quadrants and labeled as shown.

Figure 3 shows an overview of a pressure bottle instrumented with arrays of multi-axis fiber grating strain sensors, enabling damage to be assessed quickly and efficiently with resolution and accuracy comparable or better than eddy current or ultrasonic methods at a fraction of the time and cost. The purpose of the demonstration described in this paper was to introduce the beginning of a process to determine the potential of these arrays for locating and quantify damage. Specific objectives of the demonstration were to investigate the ability of the multi-axis fiber grating sensors to locate and identify damage, establish the ability of the sensors to sense damage at various ranges and depths through the use of optical fiber lines embedded into various composite layers. Other objectives included the investigation of changes/damage during pressure cycling and strains seen in process/cure during manufacturing.

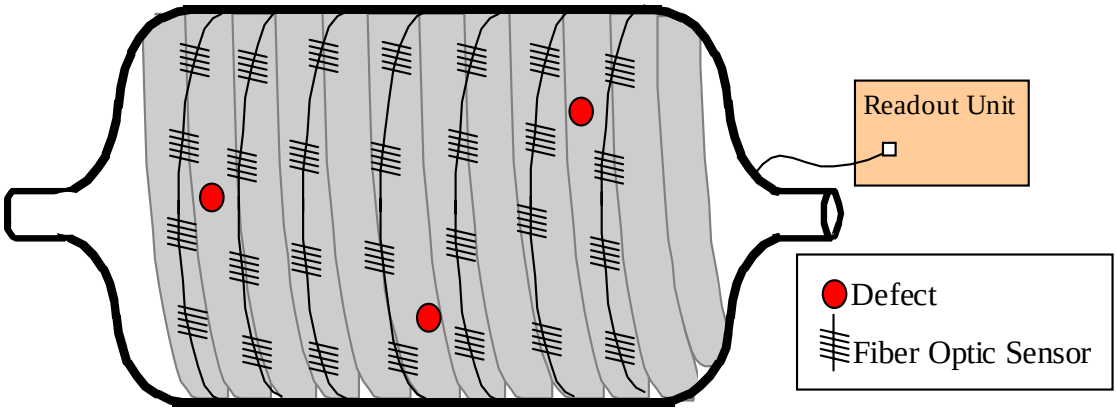

Figure 3. The end objective is to have a series of multi-axis fiber grating sensors wound into a bottle to assess damage similar to eddy current or ultrasonics at a small fraction of the time and cost.

In Quadrant 1, two Teflon tape defects and two cut tow damage sites were investigated. For one set of Teflon tape defect and cut tow damage, an array of six fiber grating sensors were used to study the effects of spatial offsets through cure, pressure cycles, and impacts (see Figure 4). In addition, a second set of Teflon and cut tow defects were studied in Quadrant 1 (see Figure 5). In this second case to measure 'shading', fiber gratings were arranged so that the optical fibers running parallel through the bottle could be scanned with the objective of determining if both sensors could read damage or if the closest sensor to damage blocked the second. Additionally, fiber gratings were placed in the layers above and below the damage sites to test the ability of the gratings to measure damage above and below defective layers.

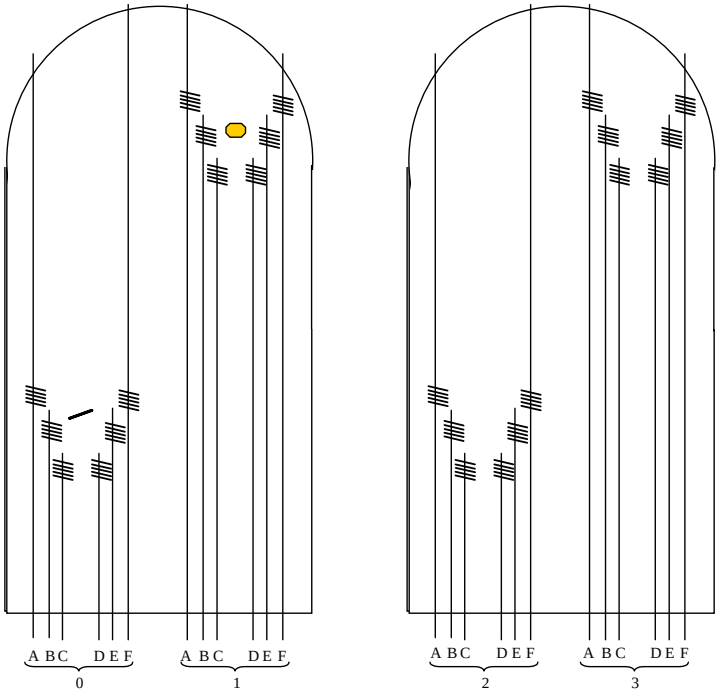

Figure 4. In Quadrant 1, six multi-axis fiber grating sensors were placed around a Teflon tape defect and a cut tow defect.

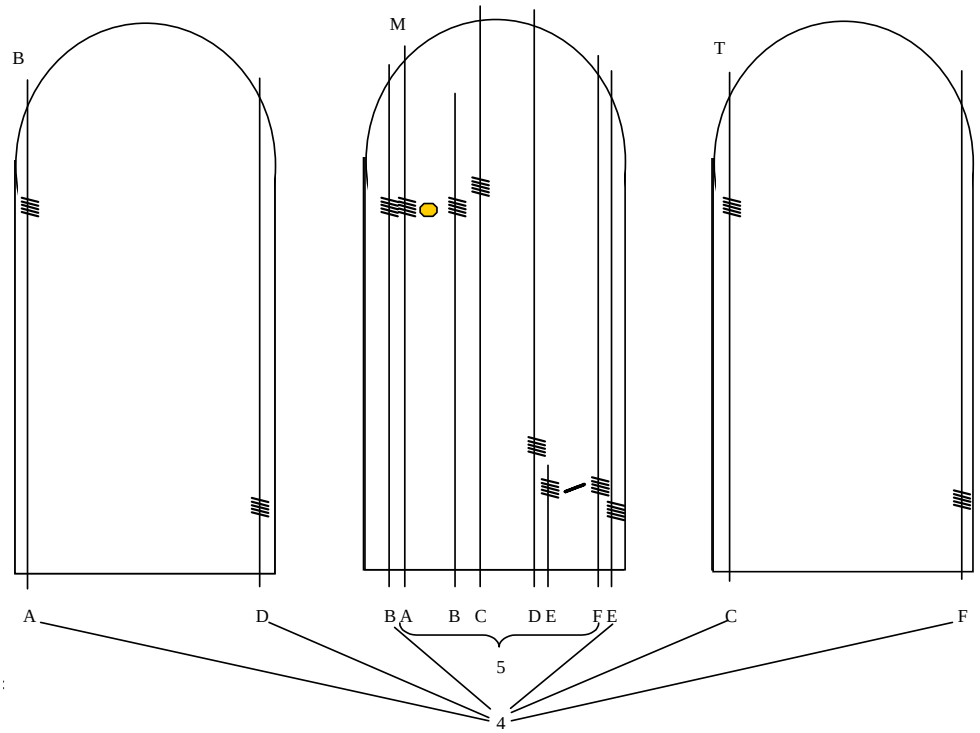

Figure 5. Fiber grating sensors were placed to purposefully induce shading effects in the area of a second Teflon tape and cut tow defect of Quadrant 1 and also to assess the sensitivity of sensors placed above and below the damage sites.

To provide a basis for comparison, eddy current and ultrasonic scans were performed after each pressure cycle and impact. Figure 6 shows the eddy current system used. Shown in Figure 7 are eddy current scans of the pressure bottle for Quadrant 1. There are three impact areas corresponding to a Teflon tape defect (upper right hand corner) and the two cut tows. Figure 8 shows a similar scan using ultrasonic techniques.

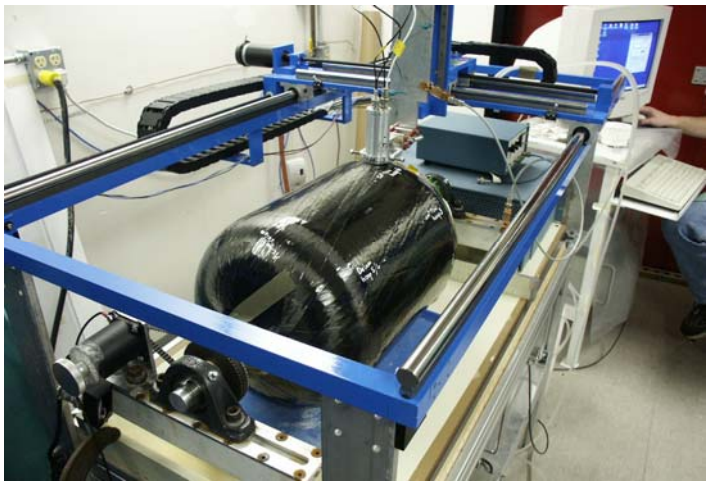

Figure 6. Eddy current scanning machine used to assess damage.

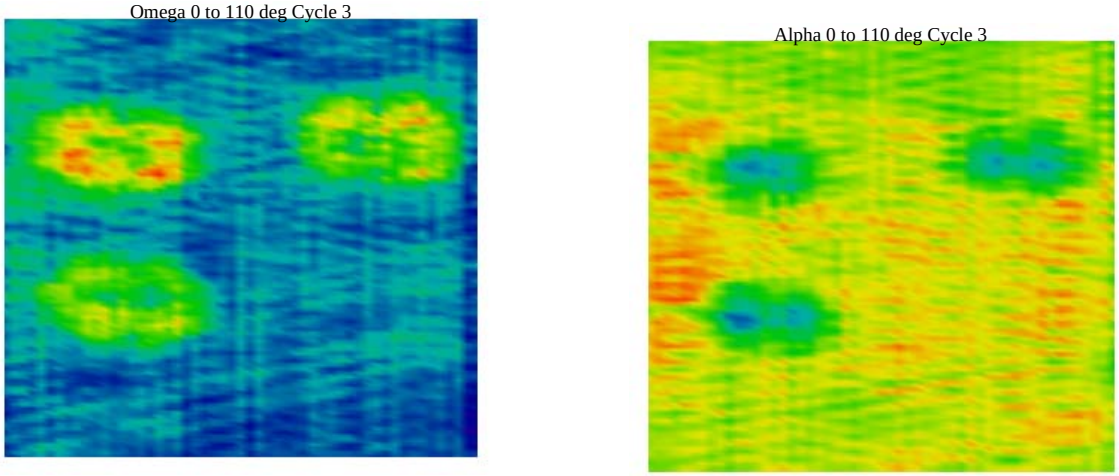

Figure 7. Eddy current scans of Quadrant 1 after the second impact and before the third pressure cycle.

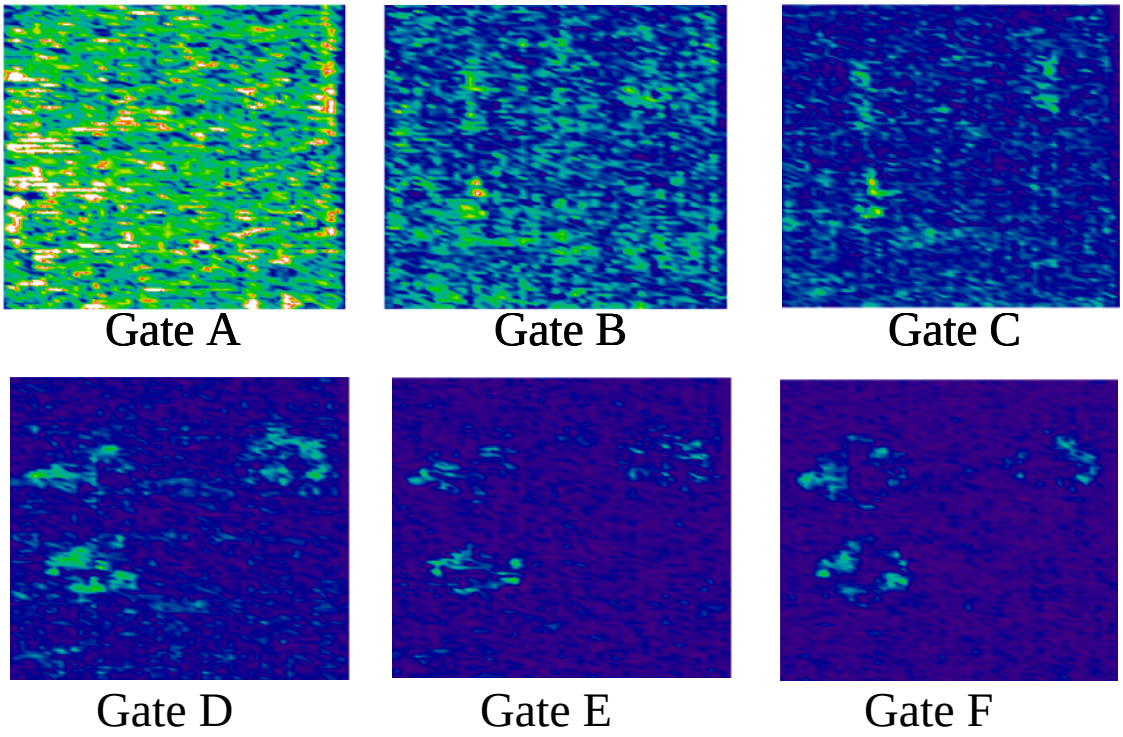

Figure 8. Ultrasonic time/gate scans through successively deeper layers, down through approximately 6 plies.

Figure 9 shows a fiber grating sensor in the cut tow region, approximately 5 cm from the damage site, during the manufacture cure cycle. Note that as the cure progresses over several hours, each of the peaks spread, indicating that transverse strain gradient magnitudes are increasing.

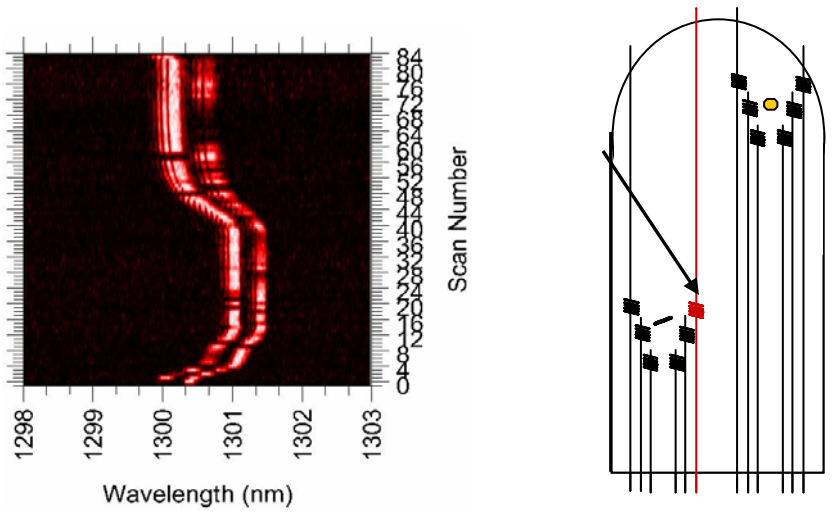

Figure 9. The fiber grating sensor indicated by the arrow near the cut tow was monitored during cure. Note the steady spread in the spectral width of the output spectrum.

Figure 10 shows another 3-D graph of data tilted to show magnitudes of the amplitude (Figure 9 is color coded for amplitude). In this case, the multi-axis fiber grating strain sensor is near the Teflon tape defect. However, there is little indication that transverse strain fields are affected in the region of the sensor.

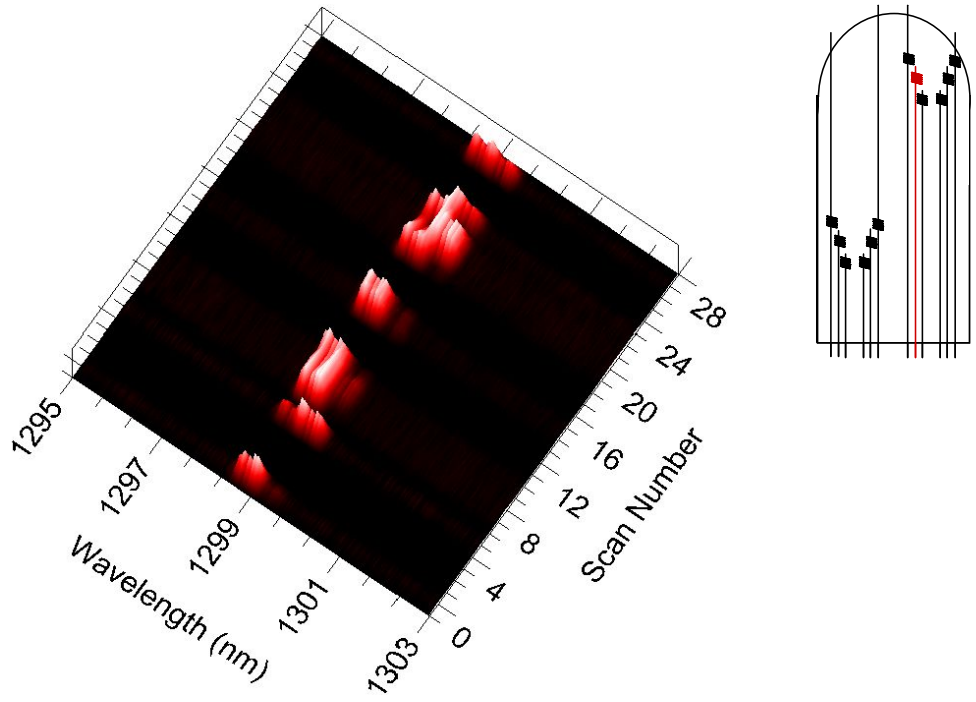

Figure 10. 3D graph of the spectrum of a multi-axis sensor during cure, near a Teflon tape defect. Note that the spectrum stays relatively uniform.

Figure 11 illustrates in 3D form three multi-axis fiber grating sensors near the Teflon tape defect that is located in the dome (in the region of Quadrant 1 where there is no evidence of damage from the eddy current or ultrasonic scans).

Figure 12 shows pressure cycles and impact-induced changes near one of the cut tow regions. In this case there are multi-axis fiber grating sensors located immediately above and below the cut tow (F and E respectively) and one multi-axis fiber grating one layer down from the damage area (D). Both D and E show very large transverse strain gradient increases. Sensor F is less dramatic although there appears to be significant transverse strain gradient growth there as well.

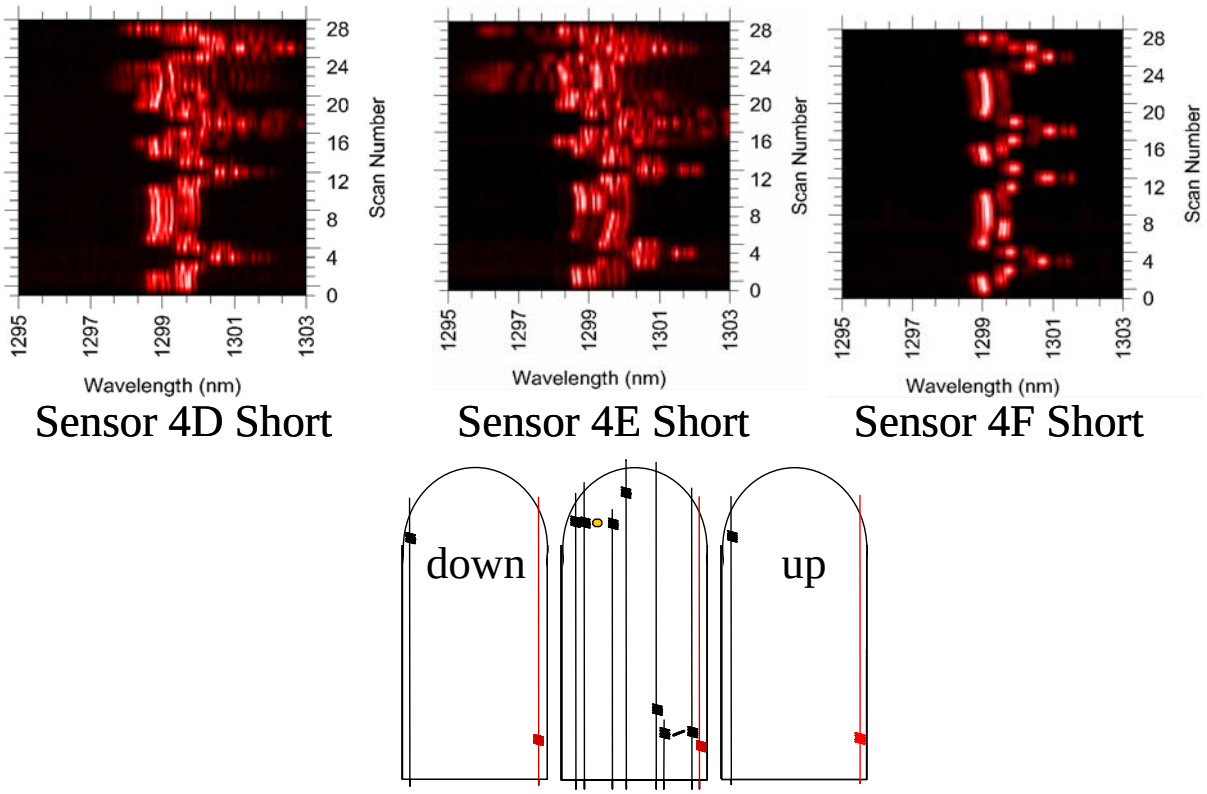

Figure 11. Damage near a cut tow from fiber gratings one layer down, in the same layer, and one layer up (respectively). In two of the cases, significant transverse strain gradients grow with pressure cycling and impacts.

In Figure 12, the pressure cycles have been removed to see the permanent effects of the growth of transverse strain gradients. Figure 12 shows a multi-axis fiber grating sensor near a cut tow (a) and another in the vicinity of a Teflon tape defect (b), which shows the typical peak-spread response of a grating as a delamination propagates across the sensor.

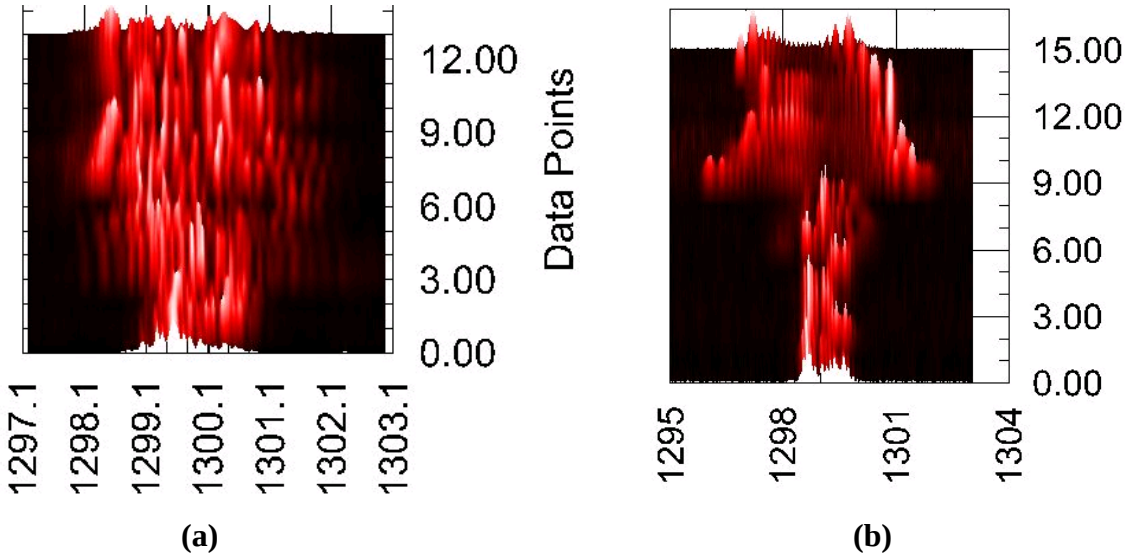

Figure 12. A multi-axis fiber grating sensor in the vicinity of a cut tow (a), and (b) a multi-axis fiber grating sensor in the vicinity of a Teflon tape defect. The dramatic shift in (b) occurs after a second impact near the defect.

The characteristic of the growth of transverse strain gradients for the cut tow and the Teflon tape defect are very different. After cure the evidence of significant transverse strain gradients due to the cut tow is very clear in Figure 12a. At the same time the changes in the transverse strain fields after cure in the region of the Teflon tape defect are not evident in Figure 12b. Pressure cycling and impacts cause the damage site to propagate. For the case of cut two in Figure 12a this results in a gradual broadening of the spectral profiles due to transverse and axial strain gradients. The case of the Teflon tape defect shown in Figure 12b is very different. Here the transverse strain gradients appear to be isolated from the multi-axis fiber grating sensor until a threshold damage condition is reached. At this point a very large transverse strain signal appears that appears to be gradually relieved as further damage changes the strain field conditions. The magnitude of the transverse strain gradients starts decreasing with additional damage in both the cut tow and Teflon tape defect regions likely is due to the composite starting to break up around the region of the multi-axis fiber grating sensor.

DAMAGE READ-OUT SYSTEM

There are a number of ways to use the information associated with the transverse strain field information to create a damage assessment system. Since the axes of the multi-axis fibers may be aligned in the plane and perpendicular to the plain of the cylinder, a rotational direction of the damage may be determined. Shifts in overall damage levels may be determined by measuring the overall spectral width of the output signal. A color-coded system is being devised and used to track the changing damage state of the tank.

Figure 13 illustrates an interface that has been developed to allow an end user to view changes in the damage state various cut tow and Teflon tape regions of the test article through pressure cycling and impact.

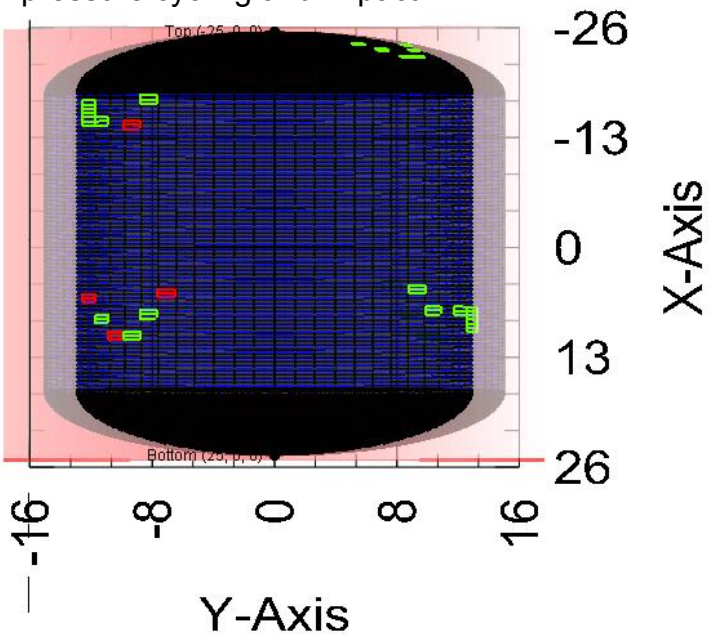

Figure 13. As pressure cycling and impacts change the integrity of the vessel wall, the strain fields measured by the multi-axis fiber grating strain sensors quantify and pinpoint damage to the structure.

SUMMARY

Strain imaging using multi-axis fiber grating sensors may be used to assess the location and type of damage experienced by a cylindrical pressure vessel. Transverse strain gradients allow end users to track the type of damage as well as the location. Further refinements and extensions of the strain imaging system are in the process of being developed although early results appear very promising.

ACKNOWLEDGEMENTS

Blue Road Research acknowledges funding support for this research effort from the SBIR Phase II Air Force Contract F04611-02-C-0007 with portions from SBIR Phase II Air Force Contract F33615-02-C-5043.

REFERENCES

1. E. Udd, W. Schulz, J. Seim, E. Haugse, A. Trego, P. Johnson, T. Bennett, D. Nelson, A. Makino, “Progress on Multidimensional Strain Field

Measurements using Fiber Optic Grating Sensors", Sensors Expo Proceedings, Anaheim, p. 203, 2000.
2. E. Udd, W.L. Schulz, J.M. Seim, A. Trego, E. Haugse, P.E. Johnson, "Use of Transversely Loaded Fiber Grating Strain Sensors for Aerospace Applications", SPIE Proceedings, Vol. 3994, p. 96, 2000.
3. W.L. Schulz, E. Udd, J.M. Seim, A. Trego, I.M. Perez, "Progress on Monitoring of Adhesive Joints using Multiaxis Fiber Grating Sensors", SPIE Proceedings, Vol. 3991, p. 52, 2000.